Physica E 83 (2016) 345–348

Contents lists available at ScienceDirect

Physica E

journal homepage: www.elsevier.com/locate/physe

# Transport properties in a monolayer graphene modulated by the realistic magnetic field and the Schottky metal stripe

Jian-Duo Lu *, Yun-Bao Li, Hong-Yu Liu, Shun-Jin Peng, Fei-Xiang Zhao

*Hubei Province Key Laboratory of Systems Science in Metallurgical Process, Wuhan University of Science and Technology, Wuhan 430081, China*

## HIGHLIGHTS

- Transport is studied in a graphene modulated by realistic magnetic field and electrical barrier.
- Electron transport properties are strikingly controlled by the incident angle of carriers.
- Electron transport properties depend on the height, position as well as width of the barrier.
- These are very helpful for designing the graphene-based nanodevices.

## GRAPHICAL ABSTRACT

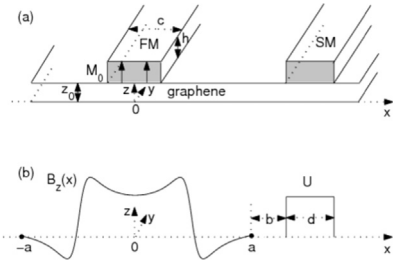


## ARTICLE INFO

*Article history:*
Received 12 February 2016
Received in revised form
1 April 2016
Accepted 5 April 2016
Available online 7 April 2016

*Keywords:*
Graphene
Electron transmission
Dirac equation
Semiconductors

## ABSTRACT

Based on the transfer-matrix method, a systematic investigation of electron transport properties is done in a monolayer graphene modulated by the realistic magnetic field and the Schottky metal stripe. The strong dependence of the electron transmission and the conductance on the incident angle of carriers is clearly seen. The height, position as well as width of the barrier also play an important role on the electron transport properties. These interesting results are very useful for understanding the tunneling mechanism in the monolayer graphene and helpful for designing the graphene-based electrical device modulated by the realistic magnetic field and the electrical barrier.



## 1. Introduction

Recently, graphene, a single-layer two-dimensional material, has attracted tremendous interest due to its experimental realization [1,2] and potential applications in various nanoelectronic devices [3–7]. Therefore, researchers began to focus on the electron transport property [8,9], which is definitely different from that found in the conventional solid-state materials [10–12]. This point can be ascribed to be that in graphene-based nanoelectronic devices, the low-energy electron could be described by the massless Dirac equation as it transmits ballistically [13–15]. Consequently, in the graphene-based structures, one can observe many interesting phenomena including the Klein tunneling [16] and the unconventional quantum Hall effect [17] as well as the minimal conductivity [18], which are absent in conventional materials.

In the meantime, in order to better design the graphene-based nanoelectronic devices, the electron transport properties in graphene are widely investigated [19–23] both experimentally and theoretically. Many researchers have focused on the electron transport properties of zigzag graphene nanoribbons (GNRs) and the possibility to control their spin conductance [24–26]. This is because GNRs have very interesting electronic properties depending on their sizes and edge shapes [27]. Furthermore, it is found that the transport properties of the massless two-

* Corresponding author.
*E-mail address:* l_j316@163.com (J.-D. Lu).

http://dx.doi.org/10.1016/j.physe.2016.04.006
1386-9477/

dimensional Dirac electrons can be controlled by the inhomogeneous magnetic fields on the nanometer scale [28–30], providing another method to the manipulation of electrons in graphene. In addition, due to the experimental realization of graphene superlattice (GSL) [31,32], the electron transport properties in the GSL have been investigated and many interesting results have been achieved [33–36].

Motivated by the above researches, in the present paper, we numerically investigate the electron transport properties of massless Dirac fermions in a monolayer graphene modulated by a ferromagnetic metal (FM) stripe and a Schottky metal (SM) stripe deposited on the top of the graphene, which has not been studied as we know. The FM stripe and SM stripe can provide a realistic magnetic field [11,12] and a electrostatic barrier [37–39], respectively, to control the electron transport properties of massless Dirac fermions. We analyze the effect of the incident angle of carriers, the height, position as well as width of the barrier on the electron transport properties including the electron transmission and the conductance. The research results are very useful for designing the graphene-based nanoelectronic devices.

## 2. Theoretical method and formulas

The motion of massless Dirac electrons in the graphene $(x, y)$ plane is considered here as sketched in Fig. 1(a). Here, the symbols $M_0$, $c$, $h$ and $z_0$ denote the magnetization, width, thickness and vertical distance to graphene plane of the FM stripe, respectively. Fig. 1(b) gives the profile of the realistic magnetic field $B_z(x)$ and the electrostatic barrier $U$. Here, the symbol $a$ is the half-width of the magnetic field, $b$, $d$ and $U$ denote the position, the width and the height of the barrier, respectively. The magnetic field can be written as [40] $\mathbf{B} = B_z(x)\mathbf{z}$ with

$$B_z(x) = B_0\left[\frac{2c(x+c/2)}{(x+c/2)^2+z_0^2} - \frac{2c(x-c/2)}{(x-c/2)^2+z_0^2}\right], \tag{1}$$

where $B_0 = M_0 h/c$, $z_0 \ll h$ and $h \ll c$. In the vicinity of the Dirac point, the low-energy excitations can be described by the following Dirac equation:

$$[v_F\sigma(\mathbf{p} + e\mathbf{A}) + U(x)\sigma_0]\psi = E\psi. \tag{2}$$

Here $v_F \approx 10^6$ m/m is the Fermi velocity of graphene, $\sigma = (\sigma_x, \sigma_y)$ is the Pauli matrix, $\mathbf{p} = (p_x, p_y)$ is the momentum operator,

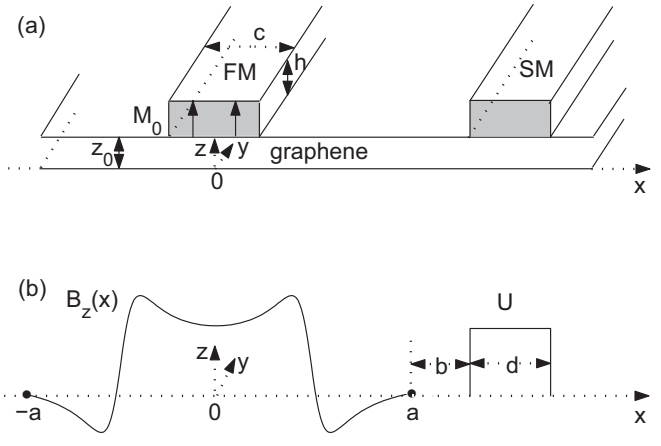


**Fig. 1.** (a) Schematic illustration of the considered monolayer graphene modulated by the realistic magnetic field and the SM stripe. The applied voltage on SM stripe provides one electrostatic barrier. (b) Simplified profiles of the realistic magnetic field $B_z(x)$ and the electrostatic barrier $U$.

$\mathbf{A} = [0, A_y(x), 0]$ with $A_y(x) = B_0 c \ln[\frac{(x+c/2)^2+z_0^2}{(x-c/2)^2+z_0^2}]$ is the magnetic vector potential given in the Landau gauge, and $\sigma_0$ is the $2 \times 2$ unit matrix. To simplify the notation, we introduce the dimensionless units: $l_{B0} = \sqrt{\hbar/eB_0}$, $E_0 = \hbar v_F/l_{B0}$, $E \to E_0 E$, $U(x) \to E_0 U(x)$, $\mathbf{B}_z(x) \to B_0\mathbf{B}_z(x)$, $\mathbf{r} \to l_{B0}\mathbf{r}$ and $\mathbf{A}(x) \to B_0 l_{B0}\mathbf{A}(x)$. For $B_0 = 0.1$ T as some typical magnetic field, we have $l_{B0} = 81.1$ nm, $E_0 = 7.0$ meV [28] and parameters of the structure are taken to be $c = 1$, $z_0 = 0.1$ and $a = 3$ [11,41].

Since the system is translational invariant along the $y$-direction and the transverse wave vector $k_y = E\sin\theta$ with $\theta$ denoting the incident angle of carriers relative to the $x$ direction in the $(x, y)$ plane is conserved [42], the wave function of the incident electrons for a given incident energy $E$ and a given incident angle $\theta$ could be written as [43]

$$\psi(x, y) = \begin{Bmatrix} \tau e^{ik_x x} + \gamma e^{-ik_x x} \\ \frac{k_x + iq}{E-U}\tau e^{ik_x x} + \frac{-k_x + iq}{E-U}\gamma e^{-ik_x x} \end{Bmatrix} e^{ik_y y}. \tag{3}$$

Here, $k_x$ is the longitudinal wave vector and $q = k_y + A_y$ satisfying $k_x^2 + q^2 = (E-U)^2$. Using the transfer-matrix method, we can obtain the transmission probability $T(E, k_y)$ [12,22]. Then, the angularly averaged conductivity at zero temperature can be calculated from the Landauer–Büttiker formula:

$$G = G_0 \int_{-\pi/2}^{\pi/2} T(E, E\sin\theta)\cos\theta\, d\theta, \tag{4}$$

where $G_0 = 2e^2 E_F L_y/(\pi h)$, $L_y$ is the width of the graphene strip along $y$-axis.

## 3. Numerical results and discussions

First, we investigate the electron transmission versus the electron energy for the different incident angles in Fig. 2(a). From the figure, one can clearly see that, with the increase of the incident angle, the vibration amplitude of the transmission curve obviously increases, and the electron transmission is strikingly suppressed. This is the result of that the electron reflection is enhanced when the incident angle increases. One also can easily see that, with the electron energy increasing, the vibration amplitude of the transmission curve rapidly decreases, and the transmission more quickly becomes perfect transmission without the oscillatory behavior for the smaller incident angle. This can be ascribed to the enhancement of the electron transmission for the higher electron energy or for the smaller incident angle. Next, we turn to study the dependence of the transport properties on the height of the barrier as illustrated in Fig. 2(b). Apparently, when the height of the barrier increases, the transmission peak obviously shifts to the higher electron energy region, and the transmission curve has a bigger oscillation magnitude. Furthermore, in the high electron energy region, with the increase of the barrier height, the transmission is more suppressed and it more quickly approaches one without the oscillation.

Second, we continue investigating the electron transport properties as a function of the electron energy in Fig. 3(a) and (b), which simulate the effect of the barrier position on the transmission and the dependence of the transmission on the barrier width, respectively. As shown in Fig. 3(a), one can apparently see that, with the increase of $b$, i.e., the barrier shifts rightwards, the transmission peak obviously shifts to the lower electron energy region, and its value strikingly decreases for about the electron energy $E < 2$. From Fig. 3(b), one can obviously see that, with the increase of the barrier width, the position of the transmission peak is almost unchanged. However, as the barrier width increases, the